IEEE Journal on Exploratory Solid-State Computational Devices and Circuits

Received 21 April 2015; revised 23 June 2015; accepted 22 July 2015. Date of publication 31 July 2015;
date of current version 14 October 2015.

Digital Object Identifier 10.1109/JXCDC.2015.2461618

Magnonic Holographic Memory: From Proposal to Device

FREDERICK GERTZ[1], ALEXANDER V. KOZHEVNIKOV[2], YURY A. FILIMONOV[2], DMITRI E. NIKONOV[3], AND ALEXANDER KHITUN[1]

[1]Department of Electrical and Computer Engineering, University of California at Riverside, Riverside, CA 92521 USA
[2]Kotel'nikov Institute of Radioengineering and Electronics, Russian Academy of Sciences, Saratov Branch, Saratov 410019, Russia
[3]Technology and Manufacturing Group, Intel Corporation, Hillsboro, OR 97124 USA

CORRESPONDING AUTHOR: A. KHITUN (akhitun@engr.ucr.edu)

This work was supported in part by the FAME Center, one of six centers of STARnet, a Semiconductor Research Corporation Program through Microelectronics Advanced Research Corporation and Defense Advanced Research Projects Agency, in part by the National Science Foundation under the NEB2020 Grant ECCS-112471 and in part by the RFBR grant 14-07-00896.

This work has supplementary downloadable material available online at http://ieeexplore.ieee.org, provided by the authors. This includes a PDF file which presents experimental data on the spin wave modulation in the single and double-cross YIG structures and the detailed explanations on the power consumption estimates. This material is 541 MB in size.

ABSTRACT In this paper, we present recent developments in magnonic holographic memory devices exploiting spin waves for information transfer. The devices comprise a magnetic matrix and spin wave-generating/detecting elements placed on the edges of the waveguides. The matrix consists of a grid of magnetic waveguides connected via cross junctions. Magnetic memory elements are incorporated within the junction, while the read-in and read-out are accomplished by the spin waves propagating through the waveguides. We present the experimental data on spin-wave propagation through NiFe and yttrium iron garnet $Y_3Fe_2(FeO_4)_3$ (YIG) magnetic crosses. The obtained experimental data show prominent spin-wave signal modulation (up to 20 dB for NiFe and 35 dB for YIG) by the external magnetic field, where both the strength and the direction of the magnetic field define the transport between the cross arms. We also present the experimental data showing parallel read-out of two magnetic memory elements via spin-wave interference. The recognition between the four possible memory states is achieved via proper adjustment of the phases of the interfering spin waves. All experiments are done at room temperature. Magnonic holographic devices aim to combine the advantages of magnetic data storage with wave-based information transfer. We present estimates on the spin-wave holographic devices performance, including power consumption and functional throughput. According to the estimates, the magnonic holographic devices may provide data processing rates higher than 1×10^{18} b/cm^2/s while consuming 0.15 mW. Technological challenges and fundamental physical limits of this approach are also discussed.

INDEX TERMS Holography, logic device, spin waves.

I. INTRODUCTION

THERE is growing interest in novel computational devices able to overcome the limits of the current complimentary metal–oxide–semiconductor (CMOS) technology and provide further increase of the computational throughput [1]. So far, the majority of the beyond CMOS proposals are aimed at the development of new switching technologies [2], [3] with increased scalability and improved power consumption characteristics over the silicon transistor. However, it is difficult to expect that a new switch will outperform CMOS in all figures of merit, and more importantly, will be able to provide multiple generations of improvement, as was the case for CMOS [4]. An alternative route to the computational power enhancement is via the development of novel computing devices aimed not to replace but to complement CMOS by special task data processing [5]. Spin-wave (magnonic) logic devices are one of the alternative approaches aimed to take the advantages of the wave interference at nanometer scale and utilize phase in addition to amplitude for building logic units for parallel data processing.

A spin wave is a collective oscillation of spins in a magnetic lattice, analogous to phonons, the collective oscillation of the nuclear lattice. The typical propagation speed of spin waves does not exceed 10^7cm/s, while the attenuation time at room temperature is about a nanosecond in the conducting ferromagnetic materials (e.g., NiFe, CoFe) and may be hundreds of nanoseconds in nonconducting materials [e.g., yttrium iron garnet $Y_3Fe_2(FeO_4)_3$ (YIG)]. Such a short

attenuation time explains the lack of interest in spin waves as a potential information carrier in the past. The situation has changed drastically as the technology of integrated logic circuits has scaled down to the deep submicrometer scale, where the short propagation distance of spin waves (e.g., tens of micrometers at room temperature) is more than sufficient for building logic circuits. At the same time, spin waves have several inherent appealing properties making them promising for building wave-based logic devices. For instance, spin-wave propagation can be directed using magnetic waveguides similar to optical waveguides. The amplitude and the phase of propagating spin waves can be modulated by an external magnetic field. Spin waves can be generated and detected by electronic components (e.g., multiferroics [6]), which make them suitable for integration with conventional logic circuits. Finally, the coherence length of the spin waves at room temperature may exceed tens of micrometers, which allows the utilization of spin-wave interference for logic functionality. It makes spin waves much more prone to scattering than a single electron and resolves one of the most difficult problems of spintronics associated with the necessity to preserve spin orientation while transmitting information between the spin-based units.

During the past decade, there have been a growing number of theoretical and experimental works exploring spin-wave propagation in a variety of magnetic structures [7], [8], the possibility of spin-wave propagation modulation by an external magnetic field [9], [10], and spin-wave interference and diffraction [11]–[15]. The collected experimental data revealed interesting and unique properties of spin-wave transport (e.g., nonreciprocal spin-wave propagation [15]) for building magnonic logic circuits. The first working spin-wave-based logic device has been experimentally demonstrated in [16]. Kostylev *et al.* [16] used the Mach–Zehnder-type current-controlled spin-wave interferometer to demonstrate output voltage modulation as a result of spin-wave interference. Later on, EXCLUSIVE-NOT-OR (NOR) and NOT-AND (NAND) gates were experimentally demonstrated utilizing a similar structure [17]. Then, it was proposed to combine spin wave with nanomagnetic logic aimed to combine the advantages of nonvolatile data storage in magnetic memory and the enhanced functionality provided by the spin-wave buses [18]. The use of spin-wave interference makes it possible to realize majority gates (which can be used as AND or OR gates) and NOT gates with a fewer number of elements than is required for transistor-based circuitry. There are also interesting architecture ideas aimed to benefit from clocked nonvolatile spin-wave circuits [19]. There were several experimental works demonstrating three-input spin-wave majority gates [20], [21]. Recently, a proof-of-concept three-terminal magnonic transistor has been demonstrated [22].

An alternative approach to spin-wave-based logic devices is to build non-Boolean logic gates for special task data processing. The essence of this approach is to maximize the advantage of spin-wave interference. Wave-based analog logic circuits are potentially promising for solving problems requiring parallel operation on a number of bits at time (i.e., image processing and image recognition). The concept of magnonic holographic memory (MHM) for data storage and special task data processing has been proposed in 2013 [23]. Recently, the first working MHM prototypes have been experimentally demonstrated [24], [25]. In [24], there were presented the results of the proof-of-concept experiment showing the possibility of parallel read-in of magnetic memory via spin-wave interference. In [25], an eight-terminal MHM was utilized for incoming data recognition. In this paper, we present the experimental data on spin-wave propagation in magnetic cross junctions, which are the basic building blocks of MHM. The rest of this paper is organized as follows. In Section II, we describe the structure and the principle of operation of MHM. Next, in Section III, we present the experimental data on spin-wave propagation in magnetic cross junctions. In addition, we present the experimental data showing one-step read-out of two magnetic memory elements via adjusting the phases of interfering spin waves. The advantages and the challenges of the magnonic holographic devices are discussed in Section IV. In Section V, we present the estimates on the practically achievable performance characteristics.

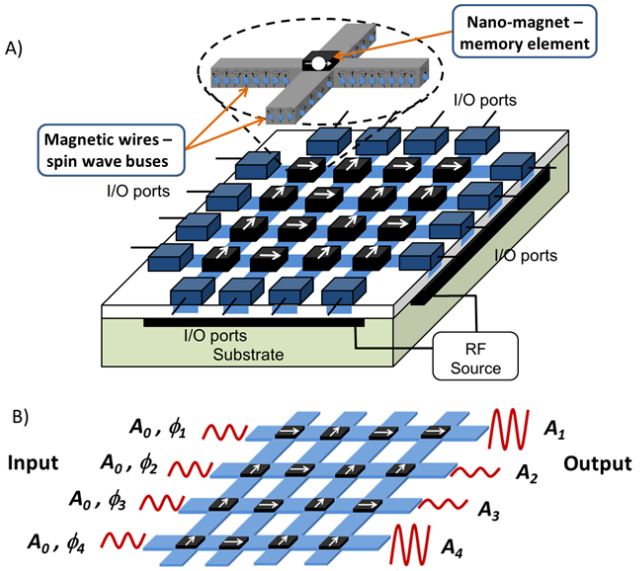

FIGURE 1. (A) Schematics of MHM consisting of a 4 × 4 magnetic matrix and an array of spin-wave generating/detecting elements. (B) Illustration of the principle of operation. Spin waves are excited by the elements on one or several sides of the matrix (e.g., left side), propagate through the matrix and detected on the other side (e.g., right side) of the structure. All input waves are of the same amplitude and frequency. The initial phases of the input waves are controlled by the generating elements. The output waves are the results of the spin-wave interference within the matrix. The amplitude of the output wave depends on the initial phases and the magnetic states of the junctions.

II. MATERIAL STRUCTURE AND THE PRINCIPLE OF OPERATION

The schematics of an MHM device are shown in Fig. 1(A). The core of the structure is a magnetic matrix consisting of

the grid of magnetic waveguides with nanomagnets placed on the top of the waveguide junctions. Without loss of generality, we have shown a 2-D mesh of orthogonal magnetic waveguides, though the matrix may be realized as a 3-D structure comprising the layers of magnetic waveguides of a different topology (e.g., honeycomb magnetic lattice). The waveguides serve as a media for spin-wave propagation—spin-wave buses. The buses can be made of a magnetic material such as YIG or Permalloy ($Ni_{81}Fe_{19}$) ensuring maximum possible group velocity and minimum attenuation for the propagating spin waves at room temperature. The nanomagnets placed on the top of the waveguide junctions act as memory elements holding information encoded in the magnetization state. The nanomagnet can be designed to have two or several thermally stable states of magnetization, where the number of states defines the number of logic bits stored in each junction [26]. The spins of the nanomagnet are coupled to the spins of the junction magnetic wires via the exchange and/or dipole–dipole coupling, affecting the phase of the propagation of spin waves. The phase change received by the spin wave depends on the strength and direction of the magnetic field produced by the nanomagnet. At the same time, the spins of the nanomagnet are affected by the local magnetization change caused by the propagating spin waves.

The input/output ports are located at the edges of the waveguides. These elements are aimed to convert the input electric signals into spin waves, and vice versa, convert the output spin waves into electrical signals. There are several possible options for building such elements using microantennas [27], [28], spin-torque oscillators [29], and multiferroic elements [6]. For example, the microantenna is a conducting contour placed in the vicinity of the spin-wave bus. An electric current passed through the contour generates a magnetic field around the current-carrying wires, which excites spin waves in the magnetic material, and vice versa, a propagating spin wave changes the magnetic flux from the magnetic waveguide and generates an inductive voltage in the antenna contour. The advantages and shortcomings of different input/output elements will be discussed.

Spin waves generated by the edge elements are used for information read-in and read-out. The difference between these two modes of operation is in the amplitude of the generated spin waves. In the read-in mode, the elements generate spin waves of a relatively large amplitude, so two or several spin waves coming in-phase to a certain junction produce magnetic field sufficient for magnetization change within the nanomagnet [18]. In the read-out mode, the amplitude of the generated spin waves is much lower than the threshold value required to overcome the energy barrier between the states of nanomagnets. So, the magnetization of the junction remains constant in the read-out mode. The details of the read-in and read-out processes are presented in [23].

The formation of the hologram occurs in the following way. The incident spin-wave beam is produced by the number of spin-wave generating elements [e.g., by the elements on the left side of the matrix, as shown in Fig. 1(B)]. All the elements are biased by the same RF generator exciting spin waves of the same frequency, f, and amplitude, A_0, while the phase of the generated waves are controlled by dc voltages applied individually to each element. Thus, the elements constitute a phased array allowing us to artificially change the angle of illumination by providing a phase shift between the input waves. Propagating through the junction, spin waves accumulate an additional phase shift, $\Delta\phi$, which depends on the strength and the direction of the local magnetic field provided by the nanomagnet, H_m

$$\Delta\phi = \int_0^r k(\vec{H}_m)dr \tag{1}$$

where the particular form of the wavenumber $k(H)$ dependence varies for magnetic materials, film dimensions, the mutual direction of wave propagation, and the external magnetic field [30]. For example, spin waves propagating perpendicular to the external magnetic field [magnetostatic surface spin wave (MSSW)] and spin waves propagating parallel to the direction of the external field [backward volume magnetostatic spin wave (BVMSW)] may obtain significantly different phase shifts for the same field strength. The phase shift $\Delta\phi$ produced by the external magnetic field variation δH in the ferromagnetic film can be expressed as follows [16]:

$$\begin{aligned} \frac{\Delta\phi}{\partial H} &= \frac{l}{d}\frac{(\gamma H)^2+\omega^2}{2\pi\gamma^2 M_S H^2} && \text{(BVMSW)} \\ \frac{\Delta\phi}{\delta H} &= -\frac{l}{d}\frac{\gamma^2(H+2\pi M_S)}{\omega^2-\gamma^2 H(H+4\pi M_S)} && \text{(MSSW)} \end{aligned} \tag{2}$$

where $\Delta\phi$ is the phase shift produced by the change of the external magnetic field δH, l is the propagation length, d is the thickness of the ferromagnetic film, γ is the gyromagnetic ratio, $\omega = 2\pi f$, and $4\pi M_s$ is the saturation magnetization of the ferromagnetic film. The output signal is a result of superposition of all the excited spin waves traveling through the different paths of the matrix. The amplitude of the output spin wave is detected by the voltage generated in the output element (e.g., the inductive voltage produced by the spin waves in the antenna contour). The amplitude of the output voltage is corresponding to the maximum when all the waves are coming in-phase (constructive interference), and the minimum when the waves cancel each other (destructive interference). The output voltage at each port depends on the magnetic states of the nanomagnets within the matrix and the initial phases of the input spin waves. In order to recognize the internal state of the magnonic memory, the initial phases are varied (e.g., from 0 to π). The ensemble of the output values obtained at the different phase combinations constitute a hologram, which uniquely corresponds to the internal structure of the matrix.

In general, each of the nanomagnets can have more than 2 thermally stable states, which makes it possible to build a multistate holographic memory device (i.e., z^N possible

memory states, where z is the number of stable magnetic states of a single junction and N is the number of junctions in the magnetic matrix). The practically achievable memory capacity depends on many factors, including the operational wavelength, coherence length, the strength of nanomagnets coupling with the spin-wave buses, and noise immunity. In Section III, we present the experimental data on the operation of the prototype 2-b MHM.

III. EXPERIMENTAL DATA

The set of experiments started with the spin-wave transport study in a single-cross structure, which is the elementary building block for 2-D MHM, as shown in Fig. 1. Two types of single-cross devices made of YIG and Permalloy ($Ni_{81}Fe_{19}$) were fabricated. Both of these materials are promising for application in magnonic waveguides due to their high coherence length of spin waves. At the same time, YIG and Permalloy differ significantly in electrical properties (e.g., YIG is an insulator and Permalloy is a conductor) and in fabrication method. YIG cross structures were made from single-crystal YIG films epitaxially grown on the top of gadolinium gallium garnett ($Gd_3Ga_5O_{12}$) substrates using the liquid-phase transition process. After the films were grown, micropatterning was done by laser ablation using a pulsed infrared laser ($\lambda \approx 1.03\ \mu$m), with a pulse duration of ~256 ns. The YIG cross junction has the following dimensions: 1) the length of the whole structure is 3 mm; 2) the width of the arm is 360 μm; and 3) the thickness is 3.6 μm. Permalloy crosses were fabricated on the top of the oxidized silicon wafers. The wafer was spin coated with a 5214E Photoresist at 4000 r/min and exposed using a Karl Suss Mask Aligner. After development, a Permalloy metal film was deposited via electron-beam evaporation with a thickness of 100 nm and with an intermediate seed layer of 10 nm of titanium to increase the adhesion properties of the Permalloy film. Liftoff using acetone completed the process. Permalloy cross junction has the following dimensions: 1) the length of the whole structure is 18 μm; 2) the width of the arm is 6 μm; and 3) the thickness is 100 nm.

Spin waves in YIG and Permalloy structures were excited and detected via microantennas that were placed at the edges of the cross arms. Antennas were fabricated from gold wire and mechanically placed directly at the top of the YIG cross. In the case of Permalloy, the conducting cross was insulated with a 100-nm layer of SiO_2 deposited via plasma-enhanced chemical vapor deposition and gold antennas were fabricated using the same photolithographic and liftoff procedure as with the Permalloy cross structures. A Hewlett-Packard 8720A vector network analyzer (VNA) was used to excite/detect spin waves within the structures using RF frequencies. Spin waves were excited by the magnetic field generated by the ac electric current flowing through the antenna(s). The detection of the transmitted spin waves is via the inductive voltage measurements as described in [31]. Propagating spin waves change the magnetic flux from the surface, which produces an inductive voltage in the antenna contour.

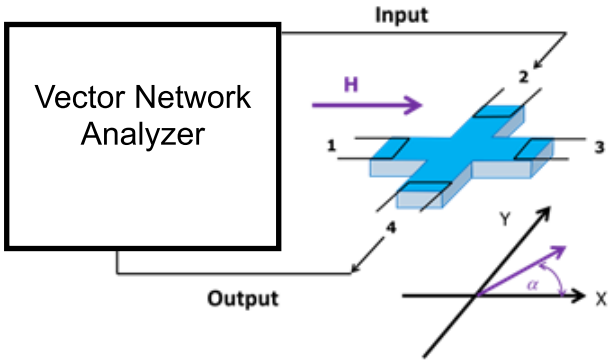

FIGURE 2. Schematics of the experimental setup for single-cross structures testing. The input and the output microantennas are connected to the Hewlett-Packard 8720A VNA. The VNA generates input RF signal and measures the S-parameters showing the amplitude and the phases of the transmitted and reflected signals. The device under study is placed inside a GMW 3472–70 electromagnet system which allows the biasing magnetic field to be varied from −1000 to +1000 Oe. The in-plane axes *x* and *y* are defined along the lines from port 1 to port 3, and from port 4 to port 2, respectively.

The VNA allowed the S-parameters of the system to be measured; showing both the amplitude of the signals as well as the phase of both the transmitted and reflected signals. Samples were tested inside a GMW 3472–70 electromagnet system which allowed the biasing magnetic field to be varied from −1000 to +1000 Oe. The schematics of the experimental setup for spin-wave transport study in the single-cross structures are shown in Fig. 2.

First, we studied the spin-wave propagation between the four arms of the Permalloy cross structure, as shown in Fig. 3(A) and (B), under different bias magnetic fields. The input/output ports are numbered from 1 to 4 starting at the 9 o' clock position and then enumerated sequentially in along a clockwise direction. In order to define the angle between the external magnetic field and the direction of signal propagation, we define the x-axis along the line from port 1 to port 3, and the y-axis along the line from port 4 to port 2 propagating, as shown in Fig. 2. Spin waves were excited on port 2 (the top of the magnetic cross) and read out from port 4 (the bottom of the cross) (see Fig. 1). The graph in Fig. 3 shows the change of the amplitude of the transmitted signal as a function of the strength of the external magnetic field directed perpendicular to the propagating spin waves, as shown in Fig. 3 (inset). Hereafter, we show the relative change of the amplitude in decibels normalized to some value (e.g., to the maximum value). The normalization is needed as the input power varies significantly for Permalloy and YIG structures as well as for the type of experiment. The reference transmission level is taken at 300 Oe, where the S_{12} parameter is at its absolute maximum. At small magnetic fields below 100 Oe, a very small amplitude signal was observed. At ~150 Oe, there is a noticeable increase in the amplitude followed by a plateau in the response as the field is increased to 500 Oe. Also of interest is the response of the

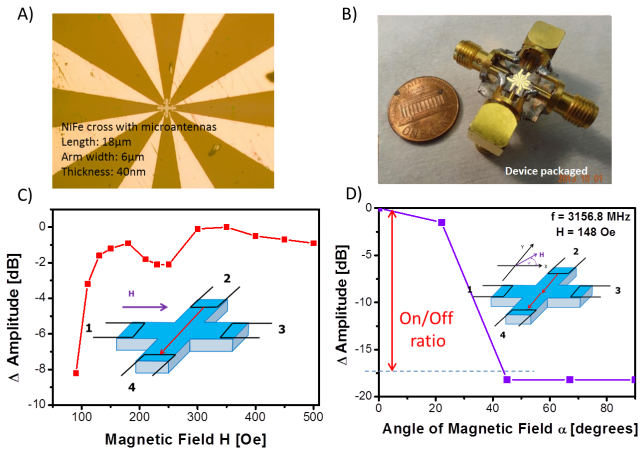

FIGURE 3. (A) Microscope image of Permalloy single-cross structure with antennas placed on the edges of the structure. The length of the whole structure is 18 μm, the width of the arm is 6 μm, and the thickness is 40 nm. (B) Photo of the packaged device with microwave input/output ports used for connection to VNA. (C) Experimental data showing the relative change of the output signal (inductive voltage) as a function of the strength of the external magnetic field. The output is normalized to the maximum output detected at 300 Oe. The signal is transmitted from port 2 to port 4, and the bias magnetic field is along the *x*-axis, as shown in the inset. The input frequency is 3.16 GHz. (D) Experimental data showing the relative change of the output signal amplitude as a function of the direction of the external magnetic field. The output is normalized to the maximum amplitude at 0° (parallel to *x*-axis). The signal is transmitted from port 2 to port 4. The measurements are taken at the different angles α of the bias magnetic field of 148 Oe, where α is defined as the angle to the *x*-axis, as shown in the inset.

signal as a function of the applied magnetic field direction. In Fig. 3(D), we present an example of the experimental data showing the influence of the direction of the bias field on spin waves transport from port 2 to port 4. The results demonstrate prominent change in the amplitude of the transmitted signal [18 dB] when the field is applied between 20° and 30°. The ability of spin-wave signal redirection between the arms of the cross junction via magnetic field is critically important for MHM operation. It allows us to control spin-wave interference by the orientation of junction magnets. In the original proposal work [23], it was assumed 6-dB signal difference in the cross-junction transmission depending on the orientation of the magnet. The obtained experimental data show even more prominent modulation, which is in favor of MHM operation. There is always certain amount of spin-wave energy scattered back from the junction. The presence of the back-scattered spin-wave signal is of minor importance for MHM as it has negligible effect on the operation of the spin-wave generating elements. The main observations of these experiments are the following: 1) spin-wave propagation through the cross junction can be efficiently controlled by the external magnetic field and 2) both the amplitude and the direction of the magnetic field can be utilized for spin-wave control. We conducted similar experiments with YIG single- and double-cross device and also observed prominent signal modulation. The details are presented in the supplementary materials online.

Concluding on the spin-wave transport in the Permalloy and YIG single-cross structures, prominent signal modulation has been observed in both cases. For the chosen parameters, the operation frequency is slightly higher for YIG structure (~5 GHz) than for Permalloy (~3 GHz). The speed of signal propagation is slightly faster in Permalloy (3.5×10^6 cm/s) than in YIG (3×10^6 cm/s). The difference in the spin-wave transport can be attributed to the differences between the intrinsic material properties of YIG and Permalloy as well as the difference in the cross dimensions. It is important to note that in both the cases, the level of the power consumption was at the microwatt scale (e.g., 0.1–1 μW for Permalloy and 0.5–5 μW for YIG) with no feasible effect of microheating on the spin-wave transport. The summary of the experimental findings for Permalloy and YIG single-cross junctions cab be found in Table 1.

TABLE 1. Summary of experimental results for Py and YIg crosses.

Table I	Permalloy	YIG
Cross dimensions	L=18μm, w=6μm, d=100nm	L=3mm, w=300μm, d=3.8μm
Operational Frequency	3GHz-4GHz	5GHz-6GHz
SW group velocity	3.5×10^6 cm/s	3.0×10^6 cm/s
Maximum On/Off ratio	20dB	35dB
Power consumption	0.1μW-1μW	0.5μW-5μW

Finally, we conducted experiments to demonstrate possibility of one-step information read-out via spin-wave interference. In the preceding work [24], we presented the collection of data—holographic images, corresponding to the different configurations of image, one has to carry out multiple measurement (~100 per hologram) detecting inductive voltage for different combinations of input phases of spin waves. The problem is ever increasing for pattern recognition [25], where all possible input phase combinations have to be checked. In practical applications, it is important to accomplish read-out in one step. In this paper, we present the experimental data showing the possibility of recognizing four possible configuration of magnets in one measurement. Two micromagnets made of cobalt magnetic film were placed on the top of the junctions of the double-cross YIG structure. The schematic of the double-cross structure with micromagnets attached is shown in Supplementary materials Fig. 2S. The length of each magnet is 1.1 mm and the width is 360 μm, and each magnet has a coercivity of 200–500 Oe. For the test experiments, we used four mutual orientations of micromagnets, where the magnets are oriented parallel to the axis connecting ports 1–6, or the axis connecting 2–4; and two cases

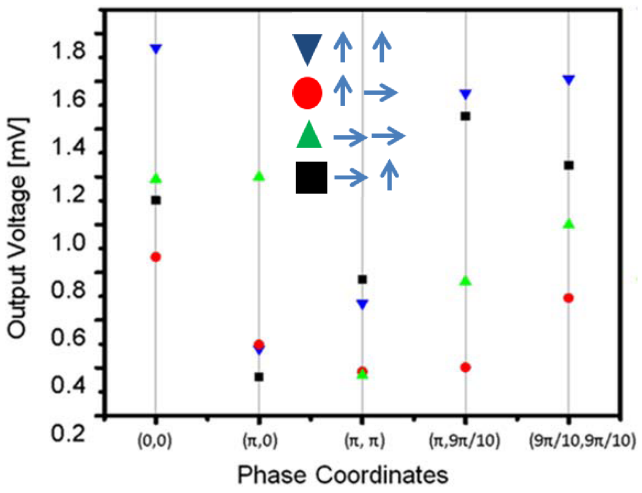

FIGURE 4. Collection of experimental data showing the output of the double-cross YIG structure with micromagnets placed on the top of the junctions. The phase coordinates show the combination of the initial phases of the spin waves, where Phase 1 and Phase 2 are defined the same way as in Fig. 2S in the Supplementary materials (i.e., 0,π) means that the spin waves generated in the ports 2,4 and 3,5 have a-π difference in the initial phase. The markers of different shapes and colors correspond to the different magnetic configurations as illustrated on the right side. All results are obtained at room temperature.

when the micromagnets are oriented in the orthogonal directions.

Fig. 4 shows the experimental data: output inductive voltage for different configurations of magnets. Markers of different shapes and colors in the legend of Fig. 4 represent the direction of the north end of the micromagnet. The output voltage varies significantly for different magnet configurations and the spin-wave phase combinations. It appears possible to recognize four states by just one measurement [e.g., (0,0) phase combination]. It is also possible that different magnetic states provide almost the same output [e.g., parallel and orthogonal magnet configurations measured at (π,0) phase combination]. The main observation we want to emphasize is the feasibility of parallel read-out and reconstruction of the magnetic state via spin-wave interference. As one can see from the data in Fig. 4(b), it is possible to distinctly identify the magnetic states of multiple magnets in just one measurement. The maximum of number of magnets depends on the detector resolution and the number of output ports used for recognition. For most of the practical applications, it is sufficient to recognize just two voltage levels per output port. We would like to emphasize that all experiments reported in this section are done at room temperature.

IV. DISCUSSION

The obtained experimental data show the practical feasibility of utilizing spin waves for building magnonic holographic logic devices and help to illustrate the advantages and shortcomings of the spin-wave approach. Of these results, there are several important observations we wish to highlight.

First, spin-wave interference patterns produced by multiple interfering waves are recognized for a relatively long distance (more than 3 mm between the excitation and detection ports) at room temperature. Despite the initial skepticism [32], coding information into the phase of the spin waves appears to be a robust instrument for information transfer showing a negligible effect to thermal noise and immunity to the structures imperfections. This immunity to the thermal fluctuations can be explained by considering that the flicker noise level in ferrite structures usually does not exceed −130 dBm [33]. At the same time, spin waves are not sensitive to the structure's imperfections, which have dimensions much shorter than the wavelength. These facts explain the good agreement between the experimental and theoretical data (as shown in Fig. S3 in the supplementary materials online).

Second, spin-wave transport in the magnetic cross junctions is efficiently modulated by an external magnetic field. Spin-wave propagation through the cross junction depends on the amplitude as well as the direction of the external field. This provides a variety of possibilities for building magnetic field-effect logic devices for general and special task data processing. Boolean logic gates such as AND, OR, NOT can be realized in a single-cross structure, where applying an external field exceeding some threshold stops/allows spin-wave propagation between the selected arms. The ability to modulate spin-wave propagation by the direction of the magnetic field is useful for the application in non-Boolean logic devices. It is important to note that in all the cases, the magnitude of the modulating magnetic field is of the order of hundreds of oersteds, which can be produced by micro- and nanomagnets.

Finally, it appears possible to recognize the magnetic state of the magnet placed on the top of the cross junction via spin waves, which introduces an alternative mechanism for magnetic memory read out. This property itself may be utilized for improving the performance of the conventional magnetic memory devices. However, the fundamental advantage of the MHM is the ability to read-out a number of magnetic bits in parallel though the obtained experimental data demonstrate the parallel read-out of just two magnetic bits. In the rest of this section, we discuss the fundamental limits and the technological challenges of building multibit magnonic holographic devices and present the estimates on the device performance.

There are two major physical mechanisms affecting the amplitude/phase of the spin wave propagating under the junction magnet: 1) interaction with magnetic field produced by the magnet and 2) damping due to the presence of the conducting material. The effect of conducting films on spin-wave propagation has been studied for MSSWs in the ferrite-metal structures [34], [35]. It was found that the strength of the spin-wave dispersion modification is defined by the critical parameter G given as the following $G = t/(q \times l_{sk}^2)$, where t is the thickness of the conducting film, q is the wave number, and l_{sk} is the skin depth.

The presence of a metallic film results in a prominent spin-wave dispersion modification for $G > 3$, if the width of the gap between the ferrite and metallic film is less than the wavelength. Spin wave is completely damped in the range $1/3 < G < 3$ due to the excessive absorption by the conducting electrons. The effect vanishes for $G < 1/3$. In our experiments, we used junction magnets made of cobalt with the thickness of 50 nm (bulk electric conductivity $\sigma \approx 1.6 \times 10^7$ S/m), which correspond to $l_{sk} \approx 1.5$ μm. The range of wave numbers q is restricted by the size of the sample $Lq > \pi/L > 10$ cm^{-1}, and by the width of the microantennas $W \approx 30$ μm, $q < \pi/W < 1000$ cm^{-1}. In all experiments, the range of the wave numbers is confined within the following range: 10 cm^{-1} $< q <$ 1000 cm^{-1}, which, in turn, corresponds to the range for parameter G: $0.002 < G < 2$. It should be noted that (3) has been derived for an infinite ferrite waveguide, which ignores the effect of space confinement. Considering the real dimensions of the YIG substrate 3.6 μm, we obtain the minimum boundary for $q \approx 80$ cm^{-1}. Thus, we have $G < 1/3$ (negligible effect of spin-wave dispersion modification due to the losses) for all experiments. In general, there may be other physical phenomena contributing to the spin-wave dispersion modification in a magnetic cross structure. The development of MHM devices will require a great deal of efforts in the theoretical study and numerical modeling of spin-wave transport in magnetic nanostructures.

We note that the functionality of the demonstrated holographic memory is different from a usual RAM. It contains both data written into nanomagnets and compared with data read-in as spin waves. The novelty of this paper lies in the operation of holographic spin waves. Writing nanomagnets can be performed using traditional methods, such as spin-transfer torque or magnetoelectric switching. Since the nanomagnets are written infrequently, this is not the limiting operation. In our demonstration, we accomplished writing of the nanomagnets during fabrication and demonstrated the read-out using spin waves.

In order to make a multibit magnonic holographic devices, the operating wavelength should be scaled down below 100 nm [23]. The main challenge with shortening the operating wavelength is associated with the building of nanometer-scale spin-wave generating/detecting elements. There are several possible ways of building input/output elements using microantennas [31], spin-torque oscillators [29], and multiferroic elements [6]. So far, microantennas are the most convenient and widely used tool for spin-wave excitation and detection in ferromagnetic films [36]. Reducing the size of the antenna will lead to the reduction of the detected inductive voltage. This fact limits the practical application of any types of conducting contours for spin-wave detection. The utilization of spin-torque oscillators makes it possible to scale down the size of the elementary input/output port to several nanometers [37]. The main challenge for the spin-torque oscillators approach is to reduce the current required for spin-wave generation. More energetically efficient is the two-phase composite multiferroics comprising piezoelectric and magnetostrictive materials [38]. An electric field applied across the piezoelectric produces stress, which, in turn, affects the magnetization of the magnetoelastic material. The advantage of the multiferroic approach is that the magnetic field required for spin-wave excitation is produced via magnetoelectric coupling by applying an alternating electric field rather than an electric current. For example, in Ni/Lead Magnesium Niobate (PMN)-Lead Titanate (PT) synthetic multiferroic reported in [39], an electric field of 0.6 MV/m has to be applied across the PMN-PT in order to produce 90° magnetization rotation in nickel. Such a relatively low electric field required for magnetization rotation translates in ultralow power consumption for spin-wave excitation [18]. At the same time, the dynamics of the synthetic multiferroics, especially at the nanometer scale, remains mostly unexplored.

To benchmark the performance of the magnonic holographic devices, we apply the charge-resistance approach as developed in [40]. The details of the estimates and the key assumptions are given in the supplementary materials. According to the estimates, MHM device consisting of 32 inputs, with a 60-nm separation distance between the inputs would consume as low as 150 μW of power or 72 fJ/computation. At the same time, the functional throughput of the MHM scales proportional to the number of cells per area/volume and exceeds 1.5×10^{18} b/cm^2/s for a 60-nm feature size. Image recognition and processing are among the most promising applications of magnonic holographic device exploiting its ability to process a large number of bits/pixels in parallel within a single core.

There are many questions on spin-wave transport (e.g., in magnetic crosses), which remain mostly unexplored. For instance, the mechanism of spin-wave splitting between the orthogonal arms is not well understood. To the best of our knowledge, there is no theoretical work explaining the observed spin-wave propagation in magnetic crosses. It would be of great interest to study the dynamics of spin-wave redirection depending on the geometry of the cross. It may be expected that the amplitude/phase of the redirected (bended) spin wave depends on the wavelength/size ratio, the material properties of the cross, and magnetic field produced by the nanomagnet. In addition, in this paper, we attribute the change in the interference pattern to the different phase shifts accumulated by the spin waves propagating under the nanomagnets of different orientations, i.e., (1) and (2). A real picture may be much more complicated due to the difference in amplitudes, which may arise to the different factors. There is no doubt that the development of MHM devices will take a great deal of efforts including the experimental as well as theoretical studies.

V. CONCLUSION

The collected experimental data show rich physical phenomena associated with spin-wave propagation in single- and double-cross structures. Prominent signal modulation by

the direction, rather than the amplitude of magnetic field and the low effect of thermal noise on spin-wave propagation at room temperature are among the many interesting findings presented here. The effect of spin-wave redirection between the cross arms by the external magnetic field may be further exploited for building a variety of logic devices. Besides, spin waves appear to be a robust instrument allowing us to sense the magnetic state of micromagnets by the change in the interference pattern. Quite surprisingly, it is possible to recognize the unique holographic output for the different orientations of micromagnets in a relatively long device at room temperature. Overall, the obtained data demonstrate the practical feasibility of building magnonic holographic devices. These holographic devices are aimed not to replace but to complement CMOS in a special type data processing, such as speech recognition and image processing. According to the estimates, scaled-magnonic holographic devices may provide more than 1×10^{18} b/cm^2/s data processing rate while consuming less than 0.2 mW of energy. The main technological challenges are associated with the scaling down the operating wavelength and building nanometer scale spin-wave generating/detecting elements with spin-torque oscillators and multiferroics being among the most promising solutions. At the same time, it is expected that reducing the operating wavelength will make the spin waves more sensitive to structure imperfections. The development of scalable magnonic holographic devices and their incorporation with the conventional electronic devices may pave the road to the next generations of logic devices with functional capabilities far beyond current CMOS.

REFERENCES

[1] (2011). *International Technology Roadmap for Semiconductors*. [Online]. Available: http://www.itrs.net

[2] K. Bernstein, R. K. Cavin, W. Porod, A. Seabaugh, and J. Welser, "Device and architecture outlook for beyond CMOS switches," *Proc. IEEE*, vol. 98, no. 12, pp. 2169–2184, Dec. 2010.

[3] D. E. Nikonov and I. A. Young, "Overview of beyond-CMOS devices and a uniform methodology for their benchmarking," *Proc. IEEE*, vol. 101, no. 12, pp. 2498–2533, Dec. 2013.

[4] G. E. Moore, "Cramming more components onto integrated circuits," *Electronics*, vol. 38, no. 8, pp. 114–117, Apr. 1965.

[5] G. Bourianoff, J. E. Brewer, R. Cavin, J. A. Hutchby, and V. Zhirnov, "Boolean logic and alternative information-processing devices," *Computer*, vol. 41, no. 5, pp. 38–46, May 2008.

[6] S. Cherepov, *et al.*, "Electric-field-induced spin wave generation using multiferroic magnetoelectric cells," *Appl. Phys. Lett.*, vol. 104, no. 8, Feb. 2014, Art. no. 082403.

[7] K. Perzlmaier, M. Buess, C. H. Back, V. E. Demidov, B. Hillebrands, and S. O. Demokritov, "Spin-wave eigenmodes of permalloy squares with a closure domain structure," *Phys. Rev. Lett.*, vol. 94, no. 5, p. 057202, Feb. 2005.

[8] S.-K. Kim, K.-S. Lee, and D.-S. Han, "A gigahertz-range spin-wave filter composed of width-modulated nanostrip magnonic-crystal waveguides," *Appl. Phys. Lett.*, vol. 95, no. 8, p. 082507, Aug. 2009.

[9] Y. Au, M. Dvornik, O. Dmytriiev, and V. V. Kruglyak, "Nanoscale spin wave valve and phase shifter," *Appl. Phys. Lett.*, vol. 100, no. 17, p. 172408, Apr. 2012.

[10] G. Gubbiotti *et al.*, "Magnetic field dependence of quantized and localized spin wave modes in thin rectangular magnetic dots," *J. Phys., Condens. Matter*, vol. 16, no. 43, pp. 7709–7721, Nov. 2004.

[11] S. Mansfeld *et al.*, "Spin wave diffraction and perfect imaging of a grating," *Phys. Rev. Lett.*, vol. 108, no. 4, p. 047204, Jan. 2012.

[12] K. Perzlmaier, G. Woltersdorf, and C. H. Back, "Observation of the propagation and interference of spin waves in ferromagnetic thin films," *Phys. Rev. B*, vol. 77, no. 5, p. 054425, Feb. 2008.

[13] V. E. Demidov, S. O. Demokritov, K. Rott, P. Krzysteczko, and G. Reiss, "Mode interference and periodic self-focusing of spin waves in permalloy microstripes," *Phys. Rev. B*, vol. 77, no. 6, p. 064406, Feb. 2008.

[14] S. V. Vasiliev, V. V. Kruglyak, M. L. Sokolovskii, and A. N. Kuchko, "Spin wave interferometer employing a local nonuniformity of the effective magnetic field," *J. Appl. Phys.*, vol. 101, no. 11, p. 113919, Jun. 2007.

[15] M. Jamali, J. H. Kwon, S.-M. Seo, K.-J. Lee, and H. Yang, "Spin wave nonreciprocity for logic device applications," *Sci. Rep.*, vol. 3, p. 3160, Nov. 2013.

[16] M. P. Kostylev, A. A. Serga, T. Schneider, B. Leven, and B. Hillebrands, "Spin-wave logical gates," *Appl. Phys. Lett.*, vol. 87, no. 15, pp. 153501-1–153501-3, 2005.

[17] T. Schneider, A. A. Serga, B. Leven, B. Hillebrands, R. L. Stamps, and M. P. Kostylev, "Realization of spin-wave logic gates," *Appl. Phys. Lett.*, vol. 92, no. 2, p. 022505, 2008.

[18] A. Khitun and K. L. Wang, "Non-volatile magnonic logic circuits engineering," *J. Appl. Phys.*, vol. 110, no. 3, p. 034306, Aug. 2011.

[19] S. Dutta *et al.*, "Non-volatile clocked spin wave interconnect for beyond-CMOS nanomagnet pipelines," *Sci. Rep.*, vol. 5, p. 9861, May 2015.

[20] Y. Wu, M. Bao, A. Khitun, J.-Y. Kim, A. Hong, and K. L. Wang, "A three-terminal spin-wave device for logic applications," *J. Nanoelectron. Optoelectron.*, vol. 4, no. 3, pp. 394–397, Dec. 2009.

[21] P. Shabadi *et al.*, "Towards logic functions as the device," in *Proc. IEEE/ACM Int. Symp. Nanosc. Archit. (NANOARCH)*, Jun. 2010, pp. 11–16.

[22] A. V. Chumak, A. A. Serga, and B. Hillebrands, "Magnon transistor for all-magnon data processing," *Nature Commun.*, vol. 5, p. 4700, Aug. 2014.

[23] A. Khitun, "Magnonic holographic devices for special type data processing," *J. Appl. Phys.*, vol. 113, no. 16, p. 164503, Apr. 2013.

[24] F. Gertz, A. Kozhevnikov, Y. Filimonov, and A. Khitun, "Magnonic holographic memory," *IEEE Trans. Magn.*, vol. 51, no. 4, Apr. 2014, Art. ID 4002905.

[25] A. Kozhevnikov, F. Gertz, G. Dudko, Y. Filimonov, and A. Khitun, "Pattern recognition with magnonic holographic memory device," *Appl. Phys. Lett.*, vol. 106, no. 14, p. 142409, Apr. 2015.

[26] J. G. Alzate *et al.*, "Spin wave nanofabric update," in *Proc. IEEE/ACM Int. Symp. Nanosc. Archit. (NanoArch)*, Jul. 2012, pp. 196–202.

[27] M. Covington, T. M. Crawford, and G. J. Parker, "Erratum: Time-resolved measurement of propagating spin waves in ferromagnetic thin films," *Phys. Rev. Lett.*, vol. 92, no. 8, p. 089903, Feb. 2004.

[28] T. J. Silva, C. S. Lee, T. M. Crawford, and C. T. Rogers, "Inductive measurement of ultrafast magnetization dynamics in thin-film permalloy," *J. Appl. Phys.*, vol. 85, no. 11, pp. 7849–7862, Jun. 1999.

[29] S. Kaka, M. R. Pufall, W. H. Rippard, T. J. Silva, S. E. Russek, and J. A. Katine, "Mutual phase-locking of microwave spin torque nano-oscillators," *Nature*, vol. 437, pp. 389–392, Sep. 2005.

[30] R. W. Damon and J. R. Eshbach, "Magnetostatic modes of a ferromagnet slab," *J. Phys. Chem. Solids*, vol. 19, nos. 3–4, pp. 308–320, May 1961.

[31] M. Covington, T. M. Crawford, and G. J. Parker, "Time-resolved measurement of propagating spin waves in ferromagnetic thin films," *Phys. Rev. Lett.*, vol. 89, no. 23, pp. 237202-1–237202-4, Nov. 2002.

[32] S. Bandyopadhyay and M. Cahay, "Electron spin for classical information processing: A brief survey of spin-based logic devices, gates and circuits," *Nanotechnology*, vol. 20, no. 41, p. 412001, Oct. 2009.

[33] E. Rubiola, Y. Gruson, and V. Giordano, "On the flicker noise of ferrite circulators for ultra-stable oscillators," *IEEE Trans. Ultrason., Ferroelectr., Freq. Control*, vol. 51, no. 8, pp. 957–963, Aug. 2004.

[34] A. G. Veselov, S. L. Visotsky, G. T. Kazakov, A. G. Sukharev, and Y. A. Filimonov, "Surface magnetostatic waves in metallized YIG films" *J. Commun. Technol. Electron.*, vol. 39, no. 12, pp. 2067–2074, Dec. 1994.

[35] Y. A. Filimonov and Y. V. Khivintsev, "The interaction of surface magnetostatic and bulk elastic waves in metallized ferromagnet-insulator structure," *J. Commun. Technol. Electron.*, vol. 47, no. 8, pp. 1002–1007, Aug. 2002.

[36] T. J. Silva, C. S. Lee, T. M. Crawford, and C. T. Rogers, "Inductive measurement of ultrafast magnetization dynamics in thin-film Permalloy," *J. Appl. Phys.*, vol. 85, pp. 7849–7862, 1999.

[37] M. Madami *et al.*, "Direct observation of a propagating spin wave induced by spin-transfer torque," *Nature Nanotechnol.*, vol. 6, pp. 635–638, Oct. 2011.

[38] K. Roy, S. Bandyopadhyay, and J. Atulasimha, "Energy dissipation and switching delay in stress-induced switching of multiferroic nanomagnets in the presence of thermal fluctuations," *J. Appl. Phys.*, vol. 112, no. 2, Jul. 2012.

[39] T. Wu *et al.*, "Giant electric-field-induced reversible and permanent magnetization reorientation on magnetoelectric Ni/(011) $[Pb(Mg_{1/3}Nb_{2/3})O_3]_{(1-x)}$–$[PbTiO_3]_x$ heterostructure," *Appl. Phys. Lett.*, vol. 98, no. 1, p. 012504, 2011.

[40] A. Sarkar, D. E. Nikonov, I. A. Young, B. Behin-Aein, and S. Datta, "Charge-resistance approach to benchmarking performance of beyond-CMOS information processing devices," *IEEE Trans. Nanotechnol.*, vol. 13, no. 1, pp. 143–150, Jan. 2014.

FREDERICK GERTZ received the B.S. degree in electrical engineering from Alfred University, Alfred, NY, USA, in 2009, and the Ph.D. degree in electrical engineering from the University of California–Riverside, Riverside, CA, USA, in 2015.

He joined ZebraSci Inc., Temecula, CA, USA, in 2014, where is currently a Research Scientist with the Research and Development Division. His current research interests include industrial nanoscale inspection technologies, and tribological films and their applications to pharmaceutical device.

ALEXANDER V. KOZHEVNIKOV received the M.S. degree in semiconductors and dielectrics physics and the Ph.D. degree from Saratov State University, Saratov, Russia, in 1984 and 2011, respectively.

He joined the Saratov Department, Institute of Radio Engineering and Electronics, Russian Academy of Sciences (RAS), Saratov, in 1984. He is currently a Senior Research Associate with the Saratov Branch, Institution of RAS, Kotel'nikov Institute of Radio Engineering and Electronics, RAS, researching linear and nonlinear dynamics of spin waves in magnetic films, and layered and patterned structures. He has 21 publications and five issued patents.

YURY A. FILIMONOV received the M.S. degree in physical and quantum electronics and the Ph.D. degree in physics from the Moscow Institute of Physics and Technology, Moscow, Russia, in 1979, and the Doctor degree in physics and Mathematics degree from the Kotel'nikov Institute of Radio Engineering and Electronics, Russian Academy of Sciences (RAS), Saratov, Russia, in 2008.

He joined the Kotel'nikov Institute of Radio Engineering and Electronics, RAS, in 1982. He received a professor position in physics of magnetic phenomena in 2010. He is currently the Director with the Kotel'nikov Institute of Radio Engineering and Electronics, RAS, Saratov Branch. He has 110 publications and ten issued patents.

DMITRI E. NIKONOV (M'99–S'06) received the M.S. degree in aeromechanical engineering from the Moscow Institute of Physics and Technology, Moscow, Russia, in 1992, and the Ph.D. degree in physics from Texas A&M University, College Station, TX, USA, in 1996.

He joined Intel, Santa Clara, CA, USA, in 1998. He is currently a Principal Engineer with the Components Research Group, Hillsboro, OR, USA, where he is involved in the simulation and benchmarking of beyond-CMOS logic devices and managing research programs with universities on nanotechnology. He has 80 publications and 48 issued patents.

ALEXANDER KHITUN received the M.S. and Ph.D. degrees in applied physics and mathematics from the Moscow Institute of Physics and Technology, Moscow, Russia, in 1991 and 1995, respectively.

He joined the University of California–Riverside, Riverside, CA, USA, in 2011, where he is currently a Research Professor with the Department of Electrical and Computer Engineering, and involved in beyond-CMOS logic devices. He has over 70 scientific publications and seven issued patents.